NANO LETTERS

2005
Vol. 5, No. 3
543−548

An Organometallic Synthesis of TiO_2 Nanoparticles

Jing Tang,[†,‡] Franz Redl,[‡,§,||] Yimei Zhu,[⊥] Theo Siegrist,[#] Louis E. Brus,[†,‡] and Michael L. Steigerwald*[,†,‡]

Department of Chemistry, Department of Applied Physics and Applied Mathematics, and Materials Research Science & Engineering Center, Columbia University, New York, New York 10027, IBM, T. J. Watson Research Center, Yorktown Heights, New York 10598, Center for Functional Nanomaterials, Brookhaven National Laboratory, Upton, New York 11973, and Bell Laboratories, Lucent Technologies, 600 Mountain Avenue, Murray Hill, New Jersey 07974

Received December 3, 2004; Revised Manuscript Received January 17, 2005

ABSTRACT

We report the synthesis of TiO_2 nanoparticles that uses the low-temperature reaction of low-valent organometallic precursors. Bis(cyclooctatetraene)titanium reacts with dimethyl sulfoxide in organic solution at temperatures as low as room temperature to produce TiO_2. In the absence of any supporting ligand, the reaction gives precipitation of amorphous TiO_2 powder; however, in the presence of basic ligands such as tributylphosphine, tributylphosphine oxide and trioctylphosphine oxide, the precipitation is arrested, and chemically distinct, isolated, internally crystalline TiO_2 nanoparticles are formed.

Introduction. Transition metal oxides are a fascinating class of inorganic materials, exhibiting a wide variety of structures, properties, and phenomena. Associated with their complex structures, these materials show a gamut of interesting properties: diverse electronic, magnetic, and optical properties. Metal oxides occur in nature as many minerals and are used in many applications such as pigments, catalysts, catalyst supports, ceramics, energy storage, magnetic data storage, sensors, and ferrofluids.[1]

Nanocrystals generally display properties different from the bulk material or the atomic or molecular species from which they are derived. A key to the study of their size-dependent properties is the availability of samples of high quality, internally crystalline nanoparticles. For significant physical measurements to be made, these samples must be macroscopic, and therefore a distribution in particle sizes is inevitable. This distribution ought to be as narrow as possible, and the position of its peak as controllable as possible. In large part, these latter goals have been achieved in the cases of nanocrystals of II−VI semiconductors and some of the late transition metals and coinage metals, but, by comparison, little work has been devoted to the synthesis of surface-passivated nanoparticles of transition metal oxides, despite their scientific potential and technological importance. TiO_2 nanoparticles are of particular interest inasmuch as they have been widely used in important technological applications. The dye-sensitized TiO_2 solar cells are inexpensive and have high photon to electron conversion efficiency.[2] TiO_2 is probably the most investigated photocatalyst system and has been found to be capable of decomposing a wide variety of organics;[3] it is becoming a promising material for lithium rechargeable batteries.[4]

Syntheses of transition metal oxide nanoparticles often involve water as solvent or reactant and thus result in particles with hydroxylated surfaces that influence properties of materials significantly.[5−6] Oxide nanoparticles lacking such hydroxylated surfaces are expected to have properties that are different from their counterparts, particularly in terms of their subsequent chemical behavior. Colvin and co-workers[7] reported the first solution-based nonhydrolytic synthesis of transition metal oxide nanocrystals. Those researchers exploited "nonhydrolytic sol−gel" chemistry that had been developed previously for the manufacture of bulk titania.[8] This approach has recently been extended to zirconia,[9] hafnia, and mixed group 4 oxides.[10] Niederberger et al.[11] have developed a distinctly different method in which $TiCl_4$ reacts with benzyl alcohol; highly crystalline TiO_2 nanoparticles form at aging temperatures as low as 40 °C. These researchers have recently extended this method to prepare nanoparticles of binary oxides such as $BaTiO_3$, $BaZrO_3$, $LiNbO_3$, $SrTiO_3$, and (Ba, Sr)TiO_3.[12]

Several other syntheses of transition metal oxide nanoparticles have been developed. One class involves the

* Corresponding author. E-mail: mls2064@columbia.edu.
† Department of Chemistry, Columbia University.
‡ Materials Research Science and Engineering Center, Columbia University.
§ Department of Applied Physics and Applied Mathematics, Columbia University.
|| IBM, T. J. Watson Research Center.
⊥ Center for Functional Nanomaterials, Brookhaven National Laboratory.
Bell Laboratories, Lucent Technologies.

10.1021/nl047992h CCC: $30.25
Published on Web 02/02/2005

decomposition of metal precursor in a hot organic surfactant: metal Cupferrons have been used to make Fe_2O_3, MnO, and CuO nanoparticles;[13] the decomposition of metal acetates such as $Zn(CH_3COO)_2$, $Mn(CH_3COO)_2$ results in ZnO[14] and MnO[15] nanoparticles respectively; and the decomposition of iron (III) acetylacetonate, $Fe(acac)_3$, yields Fe_3O_4 nanocrystals.[16] Another class involves the oxidation of metal nanoparticles: Heyon et al.[17] reported that monodispersed Fe_2O_3 nanoparticles are synthesized by controllably oxidizing iron nanoparticles formed from decomposition of $Fe(CO)_5$.

As with all synthesis procedures, each of the syntheses described above has its characteristic scope and limitations. Many rely on the reactions of low-energy reagents at fairly high temperatures (for example, the reaction of $HfCl_4$ with $Hf(O^iPr)_4$ occurs at a practical rate only above 300 °C). Here we report investigations of the other extreme, viz., the reaction of intrinsically higher energy reagents at lower temperatures. While it might be expected that the internal crystallization of the metal oxide core of the nanoparticle would ultimately require high temperatures, the chemical versatility that is implicit in low-temperature processing offers the prospect of synthesizing otherwise inaccessible metastable materials. Pursuant to the exploration of low-temperature routes to refractory materials, we here report a new synthesis of TiO_2 nanocrystals that is based on the gentle oxidation of a very reactive organometallic complex of reduced titanium. The synthesis protocol used here is a chemical relative of the well-established synthesis of metal chalcogenides by the reaction of low-valent metal complexes with phosphine chalcogenides.[18] Reasoning by analogy, a low-valent organometallic complex of titanium might be expected to react with an analogous, "low-valent" source of oxygen to give TiO_2. Bis(cyclooctatetraene)titanium (Ti(COT)$_2$) and dimethyl sulfoxide (DMSO) react in this way.

Experimental Section. *General.* Unless otherwise noted, all operations were conducted with the exclusion of air and water, using either drybox or conventional Schlenk techniques. Ti(COT)$_2$ was prepared by the reduction of titanium butoxide by triethylaluminum, following the method of Breil et al.[19] Anhydrous *o*-dichlorobenzene (ODCB), dimethyl sulfoxide (DMSO), tributylphosphine (TBP), tributylphosphine oxide (TBPO), and trioctylphosphine oxide (TOPO) were used as received from Aldrich. Elemental analysis was done using energy-dispersive X-ray spectroscopy (EDS) with an EDS attachment on a LEO 1455 UP scanning electron microscope. X-ray powder diffraction (XRD) patterns were recorded using a Scintag X2 diffractometer. Low resolution transmission electron microscopy (TEM) and selected area electron diffraction was performed using a JEOL 100cx microscope (accelerating voltage 100 kV). Higher resolution structural characterization of the nanoparticles was carried out using a field emission transmission electron microscope (JEOL3000F) operated at accelerating voltage of 300 kV.

Preparation of TiO_2 Powder. Ti(COT)$_2$ (0.24 g, 0.94 mmol) was added to 30 mL anhydrous ODCB under argon, and the mixture was heated to reflux in order to dissolve the titanium reagent. The solution was cooled to approximately 120 °C and anhydrous DMSO (0.2 mL, 0.22 g, 2.8 mmol) was added via syringe. Immediately the deep red color of Ti(COT)$_2$ bleached and a fine solid deposited. The mixture was stirred for 15 min, after which the mixture was filtered to give a pale, straw-colored solid and a colorless solution. The solid was washed several times with acetone and dried in vacuo to give 77 mg of a free-flowing very pale yellow solid. (Were the reaction shown in equation 1 to occur exclusively, 100% yield of TiO_2 would be 75 mg.) This material was amorphous as shown by the absence of X-ray diffraction. The powder was heated to 450 °C in air for 2 h. The resulting powder was white, and X-ray diffraction proved the heat-treated material to be TiO_2 (anatase).

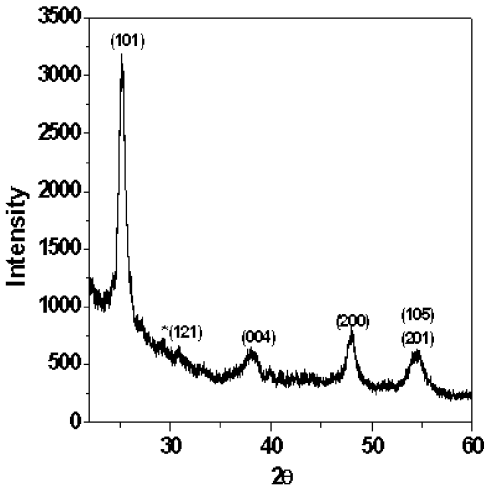

Figure 1. XRD pattern of the powder annealed at 450 °C for 2 h: * denotes brookite phase and all the other peaks correspond to anatase phase.

Preparation of TiO_2 Nanoparticles. Ti(COT)$_2$ (140 mg, 0.54 mmol) and surfactant (50 mg TBPO/0.5 mL TBP or 0.5 g TOPO) were added to 20 mL ODCB, and the mixture was heated to reflux in order to dissolve the Ti(COT)$_2$. DMSO (1.1 mmol) was added via syringe (either at room temperature or 120 °C). The color of the solution changed from dark red to pale yellow. At room temperature the color change occured over 2 days; at 120 °C the color change was immediate. At the end of the prescribed reaction time the volume of the solution was reduced by roughly 80% by the removal of solvent in vacuo. During this process the mixture was heated gently ($T = 90-100$ °C). The condensed solution was added dropwise to pentane or hexane, at which point a nearly colorless solid precipitated. This solid was collected by cetrifugation, washed several times with fresh pentane, and dried in vacuo. Both the isolated solid and the hydrocarbon/ODCB solution were analyzed and shown to contain TiO_2 nanocrystals.

Results and Discussion. We find that Ti(COT)$_2$ and DMSO react instantaneously at room temperature in ODCB, and amorphous TiO_2 precipitates rapidly (eq 1). This is shown most directly by the immediate change in color − from deep wine red to pale yellow − and the deposition of a powdery solid. The weight of the collected solid is consistent with the stoichiometry shown in eq 1, and although the powder is amorphous to X-ray diffraction, EDS of the powder shows that Ti and O are the major elements in the powder (in addition to small amounts of C, Cl, S and Al, see Supporting In-

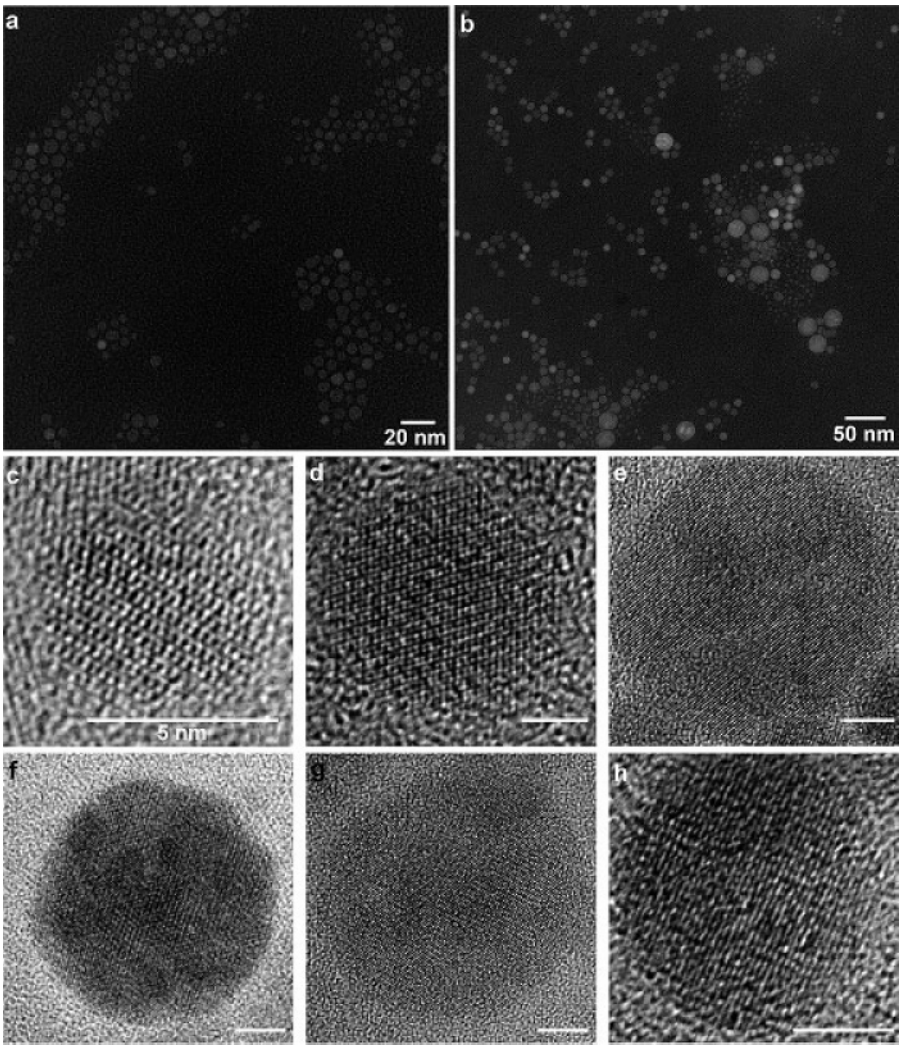

Figure 2. TEM images of particles obtained from reaction of $Ti(COT)_2$ with DMSO at room temperature using TBPO/TBP as surfactants. (a) Particles redispersed in $CHCl_3$ after being precipitated from the reaction solution by hexane. (b) Particles from the supernatant. (c−g) High-resolution TEM images of the particles. c−d are particles from sample a, which are single crystalline. e−h are the large particles from sample b. High-resolution TEM analysis reveals the various internal structures of these particles, for example, (e) is a hollow particle, (f) is a polycrystalline particle that contains different domains, while (g) and (h) are single crystalline. The scale bars in images c−h all correspond to 5 nm.

formation Figure 1S). The powder crystallizes when it is heated (450 °C, 2 h), and X-ray diffraction shows the powder to be TiO_2; primarily in the anatase form although a small amount of brookite is also indicated (Figure 1).[20] The diffraction peaks are quite broad, indicating that the crystal domains are quite small. Analysis of the (101) peak with the Debye−Scherr equation shows the average crystal domain size to be ∼11 nm.[21] These conclusions are supported by TEM. To prepare a sample for TEM, the powder was sonicated in chloroform for 30 min, and a drop of the resulting suspension was placed on a carbon film TEM grid. Owing to the absence of surface passivation, most particles aggregate (Supporting Information Figure 2Sa); nevertheless, selected area electron diffraction (SAED) from these aggregates shows many rings (Supporting Information Figure 2Sb), all but one of which can be assigned to anatase TiO_2. The single remaining peak can be assigned to the brookite form of TiO_2.

$$Ti(COT)_2 + 2OS(CH_3)_2 \rightarrow TiO_2\downarrow + 2S(CH_3)_2 + 2COT \quad (1)$$

The rapid precipitation of apparently amorphous TiO_2 is arrested when coordinating ligands (for example, TBPO/TBP) are added as synthesis auxiliaries to the ODCB solution of $Ti(COT)_2$ prior to the addition of DMSO. In this case, isolated, passivated nanocrystals of TiO_2 form. When DMSO is injected at room temperature into the solution of $Ti(COT)_2$, TBP, and TBPO, the color of the mixture changes much more slowly (over 48 h) from deep red to pale yellow, and the mixture remains essentially homogeneous. When pentane is added to the solution, a pale yellow solid precipitates. This solid can then be redispersed in $CHCl_3$, and TEM shows the solid to be composed of isolated nanoparticles of TiO_2. There is considerable distribution in size of these particles (average size 5.3 ± 1.3 nm) (Figure 2a). Even though the addition of pentane to the crude reaction mixture causes solid to precipitate, TiO_2 nanoparticles also remain in solution. The nanoparticles in this soluble fraction (Figure 2b) show an even wider distribution of sizes: particles ranging from ∼ 3 to ∼ 25 nm in diameter are present.

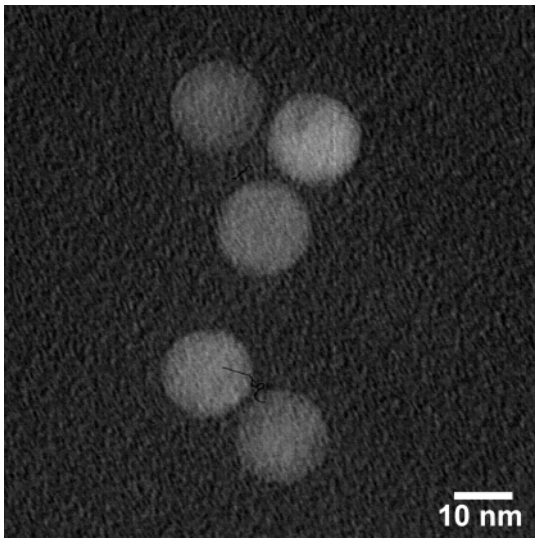

Figure 3. TEM image of TiO_2 particles obtained by injecting DMSO to $Ti(COT)_2$ at 120 °C in the presence of TOPO.

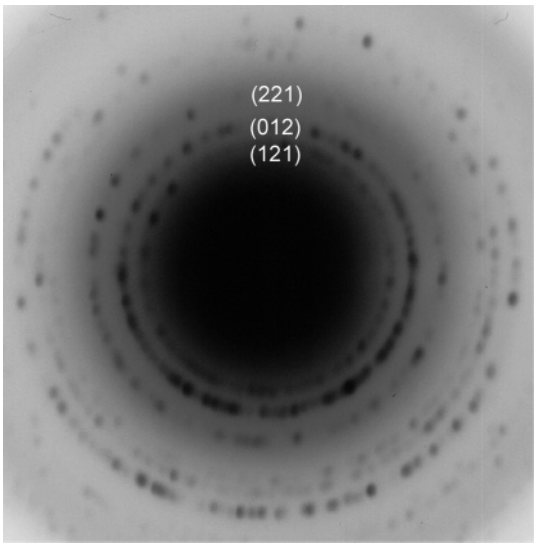

Figure 4. Electron diffraction pattern of the TiO_2 nanoparticles shown in Figure 2. These rings index well to brookite TiO_2.

The particles that precipitate are internally crystalline; high-resolution TEM characterization of these particles shows that the smaller particles are single crystalline (examples are shown in Figure 2c−d). The state of crystallinity of the particles that remain in the pentane/ODCB solution is not as simple. The largest of these "supernatant" particles show varying contrast across their diameters (see Figure 2b), which may indicate complex internal structure. This is confirmed by the high resolution TEM analysis that reveals a variety of internal structures of the large particles: large particles that appear partially hollow (Figure 2e), polycrystalline particles made up of small domains (Figure 2f), and single crystalline particles (Figure 2g−h) have all been found. The wide size distribution of the particles that are formed at room temperature indicates the particles probably grow via Ostwald ripening, in which large particles grow at the expense of small particles. We believe this is due, in turn, to the slow and continuous nucleation and growth of the particles at room temperature. The various structures of the larger nanoparticles suggest a rather complicated crystallization, growth, and agglomeration mechanism that we do not yet fully understand.

When $Ti(COT)_2$ and DMSO are combined quickly at 120 °C, again in the presence of stabilizing ligands, TiO_2 nanoparticles are formed, and the distribution in particle sizes is much narrower. Figure 3 shows a TEM micrograph of particles obtained when TOPO is used as the passivating ligand. Although the particles are quite isolated and the density of particles on the sample grid is quite low, extensive examination of the TEM grid finds that the particles are highly monodispersed and are about 15 nm in diameter. This material is very soluble in the reaction medium, and therefore we have not been able to collect a sufficient amount of it as a solid to be able to record its XRD pattern. Nevertheless, selected area electron diffraction directly proves not only the internal crystallinity but also the internal phase of the particles.

TiO_2 is known to exist in three polymorphs, namely, rutile (tetragonal), anatase (tetragonal), and brookite (orthorhombic). Rutile is the stable high-temperature phase, but anatase and brookite are common in fine-grained natural and synthetic samples.[22] When particles become smaller, the surface free energy becomes dominant, and if the surface energies of the polymorphs are sufficiently different, phase stability can be reversed for nanocrystalline particles. This has been observed in many polymorphs of other oxides such as Al_2O_3,[23] ZrO_2,[24] and Fe_2O_3,[25] etc. Zhang et al.[26] and Gribb et al.[27] observed that the synthesis of ultrafine titania resulted in anatase and/or brookite, which transformed to rutile on coarsening. Once rutile was formed, it grew much faster than anatase. From the thermodynamic analysis, they conclude that anatase becomes more stable than rutile for particle size smaller than 14 nm. Recently, Ranade et al.[28] directly confirmed the energetic crossover in nanophase polymorph stability of TiO_2 by high-temperature oxide melt drop solution calorimetry.

Selected area electron diffraction obtained on the material prepared at room tempearture is shown in Figure 4. This shows that this reaction produces TiO_2 particles largely, if not exclusively, in the brookite phase. The diffraction peak corresponding to a d-spacing of 2.9 Å can be identified with the (121) reflection in brookite; this diffraction is characteristic of brookite inasmuch as no d-spacings close to 2.9 Å exist in anatase and rutile phase.[20] Therefore, the smallest ring in the ED pattern (Figure 4), which has a d-spacing of 2.9 Å, unambiguously determines the major phase of the particles to be brookite. All the other rings match well with brookite also. The wide size distribution of the particles in the supernatant provides a good opportunity to test if a phase evolution would occur as the particle size changes from 3 to 25 nm as predicted by Zhang et al. from the thermodynamic analysis[26] and the experimental confirmation of the energetic crossover in nanophase TiO_2 by Ranade et al.[28] We examined the electron diffraction of particles of different sizes, and in each case we observed the characteristic (121) diffraction of the brookite phase. We therefore conclude that the particles are predominantly brookite. Although the

thermodynamic argument of the phase stability is found to be generally the case in experiments (for example, the amorphous TiO_2 in our case crystallizes first into anatase after calcination), the phase of the as-synthesized TiO_2 nanoparticles apparently also depends on the preparation method. Electron diffraction shows that the 15 nm nanoparticles in Figure 3 are also brookite.

We are continuing to study the mechanism(s) of this undoubtedly very complex process, and these studies are incomplete, but we offer the following preliminary considerations. First, we suggest that the process may be viewed as an assembling of "atoms", if only in the sense that the Ti and O atoms come together to form the solid-state framework without significant other chemical processes (e.g., halide/alkoxide ligand reorganizations, organic ligand isomerizations, etc.) being required. Alternatively, and perhaps more precisely, the process may be viewed as the combination of two low-valent molecular precursors. In either picture the important feature is that the ancillary ligands, COT and $S(CH_3)_2$, the chemical agents that keep the molecular precursors "molecular", simply dissociate (as closed-shell, stable molecules themselves) from the starting reagents as they become superfluous. Second, we speculate that the process is self-limiting: if a growing TiO_2 particle has its surface covered with valence-satisfied oxygen atoms, it will react only with added $Ti(COT)_2$, and then only as a two-electron donor ligand, not as an "oxygen atom" source. In this case there will be insufficient driving force for the cluster to displace both COT ligands from the incoming organometallic complex. Similarly, if the growing particle surface is covered with valence-satisfied Ti atoms, there is insufficient driving force to abstract the O from DMSO. Third, we suggest that the self-limiting nature of this reaction sequence can be defeated by the too-rapid combination of reagents. For example, consider a growing particle whose surface is covered by valence-satisfied oxygen atoms. An incoming $Ti(COT)_2$ can be in an on/off equilibrium with a two-electron donor surface oxygen atom, but if the Ti complex encounters a DMSO molecule, the fundamental polymerization reaction takes place (the COT and $S(CH_3)_2$ ligands irreversibly dissociate). If the incoming Ti and O atoms are in crystallographic register, crystalline particle growth can occur. On the other hand, if the two incoming atoms are not in register, a crystalline defect (at best) or a new nucleation site (at worst) result.

We suggest that the interplay of these three features explains the effect of temperature and added stabilizing ligands on the syntheses that we have reported here. In the absence of added stabilizing ligand, it is much more likely that the self-limiting aspect of the crystallite growth will be defeated. In one scenario, for example, a valence-satisfied surface O atom on a crystallite coordinates to a $Ti(COT)_2$ in solution, and, before the Ti can move around the surface to find a crystallographically appropriate site, it encounters a DMSO molecule, the strong covalent Ti−O bonds form, the COT and $S(CH_3)_2$ ligands dissociate, and the two new atoms are added to the crystallite at essentially arbitrary locations. If sufficient supporting ligands are present, it is less likely that the $Ti(COT)_2$ will encounter a DMSO before finding its proper (that is, lower energy) site on the growing crystal. An analogous scenario can be described in the case of higher reaction temperatures.

Conclusion. We have shown that $Ti(COT)_2$ and DMSO react readily in solution at temperatures as low as room temperature to give titania. Furthermore, when this reaction is run in the presence of appropriate coordinating ligands, the inorganic polymerization is arrested at the nanoparticle stage, and the isolated particles are internally crystalline. We have suggested that this low temperature reaction is mechanistically related to a variety of previously reported methods for the molecule-based synthesis of clusters and solid-state compounds.

Acknowledgment. We gratefully acknowledge helpful discussions with Professors Colin Nuckolls and Stephen O'Brien. This work has been primarily supported by the NSF via the MRSEC program (DMR-0213574) at Columbia University.

Supporting Information Available: EDS of the powder obtained from the reaction of $Ti(COT)_2$ with DMSO in the absence of coordinating ligands and TEM image and selected area electron diffraction of the TiO_2 particles from the 450 °C annealed sample. This material is available free of charge via the Internet at http://pubs.acs.org.

References

(1) Rao, C. N. R.; Raveau, B. *Transition metal oxides*; VCH: New York, 1995.
(2) O'Regan, B.; Grätzel, M. *Nature* **1991**, *353*, 737. Hagfeldt, A.; Grätzel, M. *Acc. Chem. Res.* **2000**, *33*, 269.
(3) Hoffmann, M. R.; Martin, S. T.; Choi, W.; Bahnemann, D. W. *Chem. Rev.* **1995**, *95*, 69 and references therein.
(4) Huang, S. Y.; Kavan, L.; Exnar, I.; Grätzel, M. *J. Electrochem. Soc.* **1995**, *142*, L142.
(5) Brinker, C. J.; Scherer, G. W. *Sol-Gel Science*; Academic Press: San Diego, 1990.
(6) Matijevic, E. *Chem. Mater.* **1993**, *5*, 412.
(7) Trentler, T. J.; Denler, T. E.; Bertone, J. F.; Agrawal, A.; Colvin, V. L. *J. Am. Chem. Soc.* **1999**, *121*, 1613.
(8) Vioux, A. *Chem. Mater.* **1997**, *9*, 2292.
(9) Joo, J.; Yu, T.; Kim, Y. W.; Park, H. M.; Wu, F.; Zhang, J. Z.; Hyeon T. *J. Am. Chem. Soc.* **2003**, *125*, 6553.
(10) Tang, J.; Fabbri, J.; Roberson, R.; Zhu, Y.; Herman, I. P.; Steigerwald, M. L.; Brus, L. E. *Chem. Mater.* **2004**, *16*, 1336.
(11) Niederberger, M.; Bartl, M. H.; Stucky, G. D. *Chem. Mater.* **2002**, *14*, 4364.
(12) (a) Niederberger, M.; Pinna, N.; Polleux, J.; Antonietti, M. *Angew. Chem., Int. Ed.* **2004**, *43*, 2270. (b) Niederberger, M.; Garnweitner, G.; Pinna, N.; Antonietti, M. *J. Am. Chem. Soc.* **2004**, *126*, 9120.
(13) Rockenberger, J.; Scher, E. C.; Alivisatos, A. P. *J. Am. Chem. Soc.* **1999**, *121*, 11595.
(14) Cozzoli, P. D.; Curri, M. L.; Agostiano, A.; Leo, G.; Lomascolo, M. *J. Phys. Chem. B* **2003**, *107*, 4756.
(15) Yin, M.; O'Brien, S. *J. Am. Chem. Soc.* **2003**, *125*, 10180.
(16) Sun, S.; Zeng, H. *J. Am. Chem. Soc.* **2002**, *124*, 8204.
(17) Hyeon, T.; Lee, S. S.; Park, J.; Chung, Y.; Na, H. B. *J. Am. Chem. Soc.* **2001**, *123*, 12798.
(18) See for example: (a) Steigerwald, M. L.; Sprinkle, C. R. *Organometallics* **1988**, *7*, 245. (b) Steigerwald, M. L.; Rice, C. E. *J. Am. Chem. Soc.* **1988**, *110*, 4228. (c) Brennan, J. G.; Siegrist, T.; Stuczynski, S. M.; Steigerwald, M. L. *J. Am. Chem. Soc.* **1989**, *111*, 9240. (d) Brennan, J. G.; Siegrist, T.; Kwon, Y.-U.; Stuczynski, S. M.; Steigerwald, M. L. *J. Am. Chem. Soc.* **1992**, *114*, 10334. (e) Murray, C. B.; Norris, D. J.; Bawendi, M. G. *J. Am. Chem. Soc.* **1993**, *115*, 8706.
(19) Breil, H.; Wilke, G. *Angew. Chem., Int. Ed.* **1966**, *5*, 898.

(20) JCPDS of TiO_2. Anatase: 21−1272; brookite: 29−1360; rutile: 21−1276.
(21) Cullity, B. D. *Elements of X-ray Diffraction*; Addison-Wesley: Reading, MA, 1978.
(22) Navrotsky, A.; Kleppa, O. J. *J. Am. Ceram. Soc.* **1967**, *50*, 626. Mitsuhashi, T.; Kleppa, O. J. *J. Am. Ceram. Soc.* **1979**, *62*, 356. Zhang, H. Z.; Banfield, J. F. *J. Phys. Chem. B* **2000**, *104*, 3481.
(23) McHale, J. M.; Auroux, A.; Perrotta, A. J.; Navrotsky, A. *Science* **1997**, *277*, 788.
(24) Garvie, R. C. *J. Phys. Chem.* **1965**, *69*, 1238.
(25) Ayyub, P.; Multani, M.; Barma, M.; Palkar, V. R.; Vijayaraghavan, R. *J. Phys. C: Solid State Phys.* **1988**, *21*, 2229.
(26) Zhang, H. Z.; Banfield, J. F. *J. Mater. Chem.* **1998**, *8*, 2073.
(27) Gribb, A. A.; Banfield, J. F. *Am. Mineral.* **1997**, *82*, 717.
(28) Ranade, M. R.; Navrotsky, A.; Zhang, H. Z.; Banfield, J. F.; Elder, S. H.; Zaban, A.; Borse, P. H.; Kulkarni, S. K.; Doran, G. S.; Whitfield, H. J. *Proc. Natl. Acad. Sci. U.S.A.* **2002**, *99*, 6476.

NL047992H